Photonic True-Time Delay Beamforming Based on Superstructured Fiber Bragg Gratings With Linearly Increasing Equivalent Chirps

Sebastien Blais, *Student Member, IEEE*, and Jianping Yao, *Senior Member, IEEE, Member, OSA*

***Abstract*—A photonic true-time delay beamforming system for phased array antennas based on superstructured fiber Bragg gratings (SFBGs) with linearly increasing equivalent chirps is proposed and demonstrated. The theory behind SFBGs with equivalent chirps is detailed and a closed-form equation for the equivalent dispersion is presented for the first time. Array factors, calculated based on the experimentally measured time delays are shown for different wavelengths of the photonic beamformer. An analysis of the errors present in the group delay responses of the fabricated SFBGs is also presented.**

***Index Terms*—Superstructured fiber Bragg gratings, equivalent chirp, photonic true-time delay beamforming, phased array antennas (PAA).**

I. Introduction

In high performance radar applications, high sensitivity, enhanced portability, increased performance of the receivers and exciters, improved resolution, large bandwidths, and wider angular scans are primary areas of performance improvement [1]–[4]. Phased array antennas (PAA) play a key role in such applications as they provide low visibility, high directivity, beam pointing agility and dynamic beam pattern shaping [5], [6]. The true time-delay (TTD) systems controlling these antennas need to answer many design constraints and performance requirements. The performance of a radar system is strongly related to its available bandwidth. In the electrical domain, this bandwidth is often limited to a few hundred megahertz. The acquisition and effective processing of multigigahertz radar signals is required to achieve improved range resolution [2], [7]–[9].

Given the recent expansion in wireless communication technology, the problems of interference, cost, maintainability, reliability, and weight grow in importance. Solutions to these problems may come in part from multiple functions provided by antennas [4], [10], [11]. Such multifunction antennas rely on their controlling circuitry to meet their operational goals. This circuitry must be easily tunable and reconfigurable. Also, an ever increasing demand for higher data rates pushes the development of systems presenting a large available bandwidth. Other design challenges include low insertion losses, low power, low production cost, light weight, and small size [12], [15].

In the past few years, TTD techniques for PAA applications have been an active area of research [9], [13]–[15]. The fact that TTD techniques eliminate the beam squint problem constitutes their most important advantage over traditional phase shifters [13]–[16]. Photonic TTD techniques are being researched as they present many advantages over electrical approaches such as an overall small size and a light weight which makes them very attractive for airborne applications, a low propagation loss which brings new possibilities to the remote control of PAAs, and immunity to electromagnetic interference (EMI) [17], [18]. The most promising advantage of photonics means to construct a TTD beamformer is the wide available bandwidth.

A promising technique to achieve photonic TTD beamforming is to use a fiber Bragg grating (FBG) prism to induce the time delay progression required [13], [17], [19], [20]. In this paper, we propose and demonstrate a photonic TTD beamforming system for a wide bandwidth PAA based on superstructured fiber Bragg gratings (SFBGs).

The use of SFBG would allow the fabrication of many time delay elements with a single uniform phase mask, a considerable advantage over the conventional approach which requires several custom-designed chirped phase masks. This is particularly attractive for TTD applications where the PAA has a large number of elements.

By adjusting the parameters of the sampling function of an SFBG, it is possible to achieve different reflection and transmission spectra, different group delay responses, and dispersion values. The fabrication of complex profiles requires only submicron precision, which can be obtained using a precise motor-driven scanning mechanical system.

This paper is organized as follows. In Section II, the system configuration using an SFBG prism for TTD beamforming is presented. An introduction to PAAs is provided in Section III. The theory behind SFBGs and a theoretical closed form equation of the dispersion in an equivalently chirped SFBG are detailed in Section IV. In Section V, a discussion on the design of the TTD beamformer and the SFBGs considered in this work is presented. In Section VI, the effects of group delay nonlinearities on the array factor is studied. Array factors of a PAA

Manuscript received January 30, 2008; revised July 24, 2008. Current version published April 24, 2009. This work was supported by the Natural Sciences and Engineering Research Council of Canada (NSERC).

The authors are with the Microwave Photonics Research Laboratory, School of Information Technology and Engineering, University of Ottawa, Ottawa, ON K1N 6N5, Canada (e-mail: jpyao@site.uOttawa.ca).

Color versions of one or more of the figures in this paper are available online at http://ieeexplore.ieee.org.

Digital Object Identifier 10.1109/JLT.2008.929421

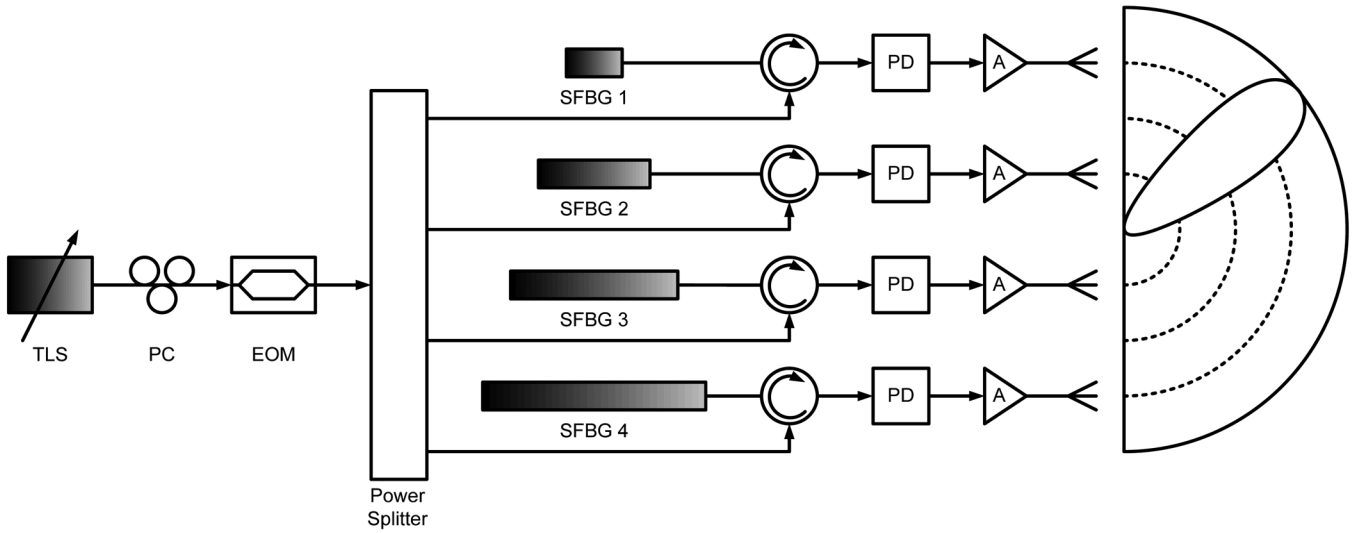

Fig. 1. System level diagram of the proposed TTD feed network for a uniformly spaced 4-element PAA using equivalent-chirped SFBGs. TLS: Tunable laser source. PC: Polarization controller. EOM: Electrooptic modulator. SFBG: Superstructured fiber Bragg grating. PD: Photodetector. A: Electrical amplifier.

calculated based on the experimental time delays are presented in Section VII. A conclusion is drawn in Section VIII.

II. System Overview

Fig. 1 presents the system level diagram of a TTD beamformer based on a SFBG prism and shows the major modules of such a system. A tunable laser source (TLS) is used to generate the optical carrier which is sent to an external electrooptic modulator (EOM) through a polarization controller (PC). The PC is properly adjusted to align the polarization direction of the lightwave from the TLS with the principal axis of the EOM, to minimize the polarization-dependent loss. At the EOM, the optical carrier is intensity modulated by a narrowband electrical signal carried by a high frequency RF carrier to be sent to the PAA. Upon entering the beamforming module, the modulated optical signal is power divided equally into four branches by a 1:4 power splitter. Each output branch is connected to a three-port optical circulator. The optical signals are then sent to the SFBG delay lines, each presenting different parameters to induce a time delay progression based on the optical wavelength. Depending on the optical wavelength, the optical signal is subjected to a different group delay as it is reflected at different locations of the SFBG. The reflected light travels back through an optical circulator to a photodetector (PD). The time delays caused by the SFBG delay lines are then translated into different beamsteering angles of the PAA.

III. PAA

Antenna arrays are essentially a group of simple antennas called array elements that are combined together to operate as a single antenna with a desired radiation pattern. The array elements may be many kind of antenna, such as dipoles, dielectric resonators or microstrip patches to only name a few. In order to shape the overall radiation pattern of the linked elements, several parameters can be controlled. These parameters include the number of elements in the array, the spatial location of each element with respect to the others, the orientation of each element as well as the parameters of the feed signals.

In a PAA, the array factor considers the combined effect of the antenna elements regardless of the type of antenna used. In the case of a PAA with its elements uniformly spaced and along a single axis, the array factor is expressed as

$$\mathrm{af}(\psi) = \frac{\sin(M\psi/2)}{M\sin(\psi/2)} \tag{1}$$

with

$$\psi = ks\cos\theta + \beta \tag{2}$$

where M is the number of elements, k is the wavenumber of the radiated signal ($k = 2\pi/\lambda_{\mathrm{RF}}$), s is the physical spacing between two adjacent antenna elements, θ is the spatial angle around the axis of orientation of the array and β is the phase progression of the electrical signals feeding the antenna elements.

In order to eliminate a phenomenon known as beam squint and to offer a wide frequency operation, beamforming based on TTD is used. Instead of inducing a phase progression in the electrical signals driving the antenna elements, the use of a time delay progression allows to steer all frequencies in the same direction. Thus, the phase progression of the electrical signals must be dependent on frequency, such as

$$\beta = 2\pi f\Delta t \tag{3}$$

where f is the frequency of the electrical signal and Δt is the time delay progression.

IV. SFBG

An SFBG, also called a sampled FBG, is composed of several sections, each containing a subgrating of a given length and a blank space. During the fabrication of an SFBG, the blank

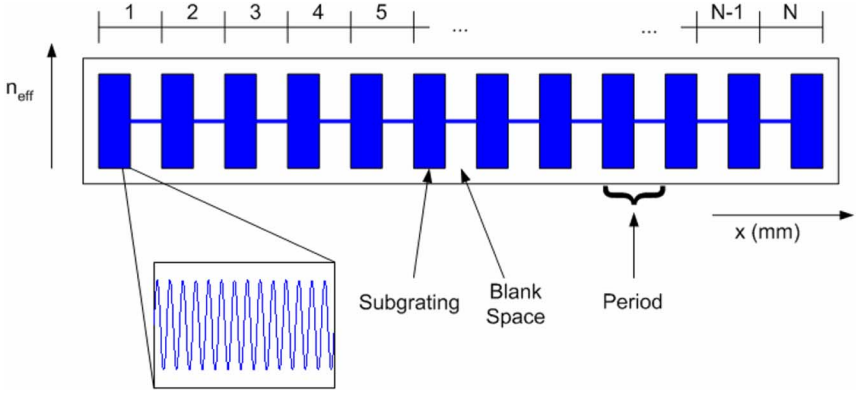

Fig. 2. Refractive index profile of an SFBG.

spaces are unexposed to UV light and, thus, they present no refractive index modulation.

The duty cycle, which is the ratio of the length of the subgrating to the period of a section (which is the sum of the length of the subgrating and the length of the blank space), can be varied to create transmission and reflection spectra with desired characteristics. By carefully designing the sampling function of the SFBG, it is possible to achieve equivalently chirped SFBGs with different equivalent chirp rates [21], [22]. Fig. 2 shows an example of a refractive index profile of an SFBG.

To design SFBGs for TTD applications, it is necessary to be able to determine the dispersion associated with the physical design parameters of these gratings. The proposed TTD beamformer based on an SFBG prism requires the design and fabrication of M SFBGs with each having a specific dispersion value. While no simple closed form expression exists to characterize the amplitude and phase response of an SFBG, it is possible to make a few approximations in order to come up with an equation describing the influence of certain parameters of the superstructure on the dispersion in a given Fourier order.

When uniform sampling is used, we have that $P(n) = P_0$. The spacing between two adjacent orders is approximated by

$$\Delta\lambda = \frac{\lambda^2}{2n_{\text{eff}}P_0} \tag{4}$$

where λ is the wavelength, n_{eff} is the effective refractive index of the fiber, and P_0 is the sampling period.

If we assume a linear chirp in the sampling function, we have

$$P(n) = P_0(1 + c_{g1}n), \qquad n = 0, 1, \ldots, N-1 \tag{5}$$

where P_0 is the initial sampling period (when $n = 0$), c_{g1} is the linear chirp coefficient and n in the sample number.

The total length of a linearly chirped SFBG can be expressed as the sum of all periods of the superstructure, as

$$L = \sum_{n} P_n \tag{6}$$

$$L = \sum_{n=0}^{N1} P_0(1 + c_{g1}n). \tag{7}$$

After a few manipulations, we get

$$L = \frac{N\,P_0}{2}\left[2 + c_{g1}(N-1)\right]. \tag{8}$$

The equivalent chirp of the superstructure can then be expressed as

$$\frac{d\lambda}{dz} = \frac{2\,m(\Delta\lambda|_{P_0} - \Delta\lambda|_{P_{N-1}})}{N\,P_0[2 + c_{g1}(N-1)]} \tag{9}$$

where $\Delta\lambda|_{P_i}$ is given by (4) and m is the Fourier order of the SFBG spectrum.

We also have that

$$P_{N1} = P_0[1 + c_{g1}(N-1)]. \tag{10}$$

By substituting (10) into (9) and after simplification, we get the following expression for the equivalent chirp:

$$\frac{d\lambda}{dz} = \frac{\lambda^2 c_{g1} m}{n_{\text{eff}}\,N\,P_0}\frac{(N-1)}{2 + 3c_{g1}(N-1) + c_{g1}^2(N-1)^2}. \tag{11}$$

It is known that the dispersion of a linearly chirped FBG can be approximated by

$$d = \frac{2\,n_{\text{eff}}}{c}\left(\frac{d\lambda}{dz}\right)^{-1} \tag{12}$$

where c is the speed of light in vacuum (3×10^8 m/s). It is then possible to approximate the dispersion in the first order of a linearly equivalent-chirped SFBG as

$$d_m = \frac{2\,N\,n_{\text{eff}}^2\,P_0^2}{c\,\lambda^2\,c_{g1}\,m} \times \left[\frac{2}{(N-1)} + 3\,c_{g1} + c_{g1}^2\,(N-1)\right]. \tag{13}$$

V. TTD Beamformer Design

Four equivalently chirped SFBGs are used in the fabrication of the TTD beamformer. Their design parameters are summarized in Table I.

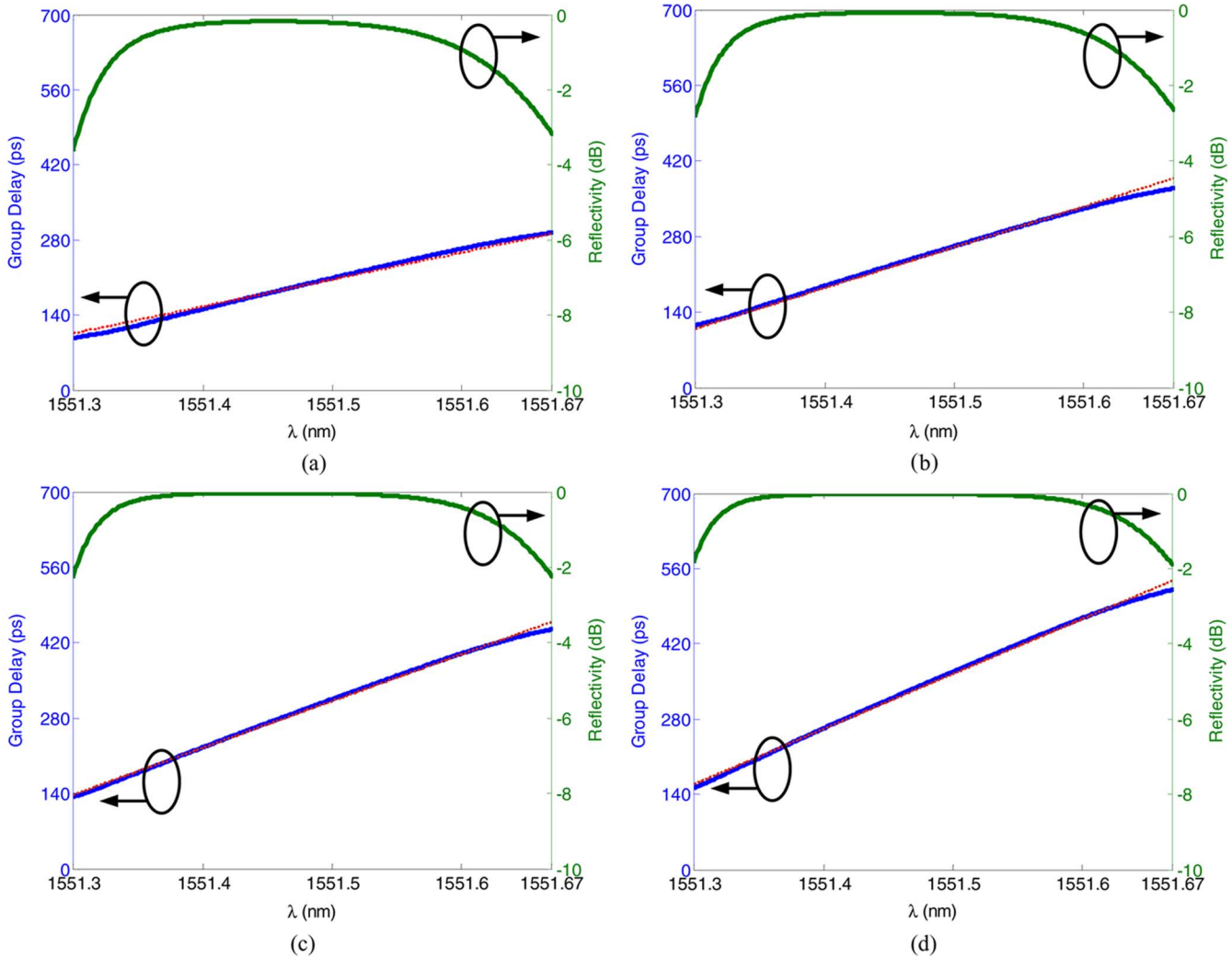

Fig. 3. Reflectivity (solid line) and simulated (solid line) and theoretical (dotted line) dispersion for the SFBG used in the true-time delay prism. The parameters of the SFBGs are given in Table I.

TABLE I
SUPERSTRUCTURED FIBER BRAGG GRATINGS PARAMETERS

	P_0 (mm)	L_s (mm)	c_{gl}	N
SFBG-1	0.6	0.3	2.564×10^{-2}	40
SFBG-2	0.6	0.3	2.040×10^{-2}	50
SFBG-3	0.6	0.3	1.695×10^{-2}	60
SFBG-4	0.6	0.3	1.449×10^{-2}	70

P_0: Initial period; L_s: Section length; c_{gl}: linear equivalent chirp parameter; N: number of periods in the superstructure.

Based on these parameters, it is possible to calculate the theoretical dispersion of these SFBGs in the -1st-order which gives the following values: SFBG-1: $d_1 = 502.0$ ps/nm; SFBG-2: $d_2 = 627.5$ ps/nm; SFBG-3: $d_3 = 753.0$ ps/nm, and SFBG-4: $d_4 = 878.5$ ps/nm. From these values, it is clear that the dispersions linearly increase with the index of the SFBGs which explains the choice of the superstructure parameters.

Fig. 3 shows the simulated amplitude and group delay responses of the SFBGs, along with the theoretical average dispersion. As no close form mathematical expression exists to characterize an SFBG, numerical simulations are usually used to evaluate the effects of the chirp coefficients on the transmission and reflection spectra of an SFBG. The transfer matrix method (TMM) is very well suited for simulation of such gratings and was used in this analysis [23].

As it can be seen, the theoretical approximation of the average dispersion matches well with the simulation results, which validates the proposed model.

With these group delay responses giving a maximal time delay progression of approximately 50 ps, it is theoretically possible to achieve beamsteering of the mainlobe of a 4-element PAA to more than $+60°$ and $-60°$ from a line perpendicular to the array axis. The beamsteering range is highly dependent on the geometry and the design of the PAA, in particular the antenna element spacing.

It should be noted that the usable beamsteering range is dependent on the frequency of the microwave signal. A high frequency signal, especially when used in a double sideband modulation scheme will occupy a large portion of the available optical

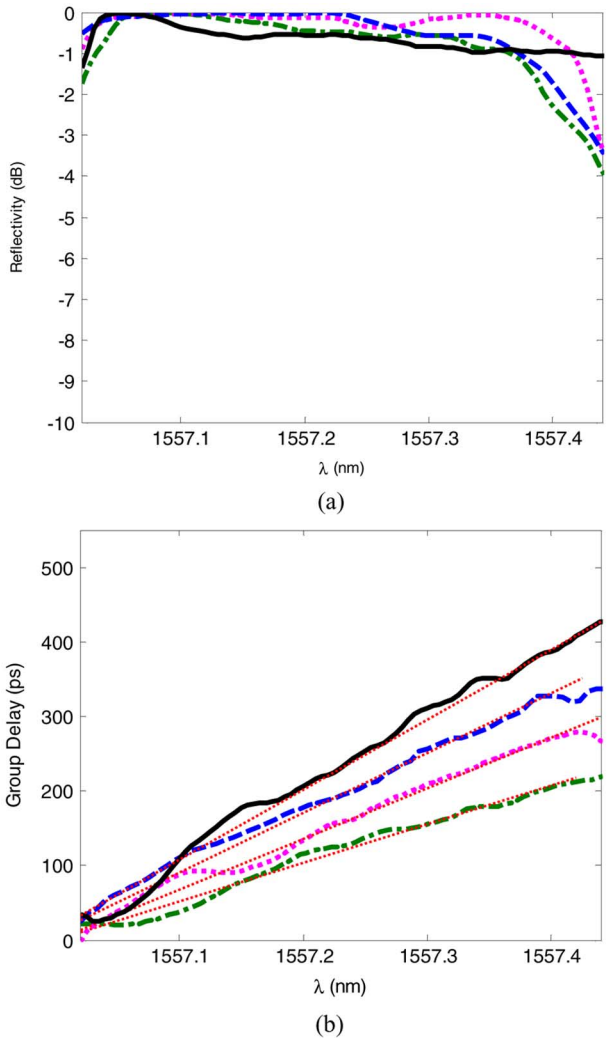

Fig. 4. (a) Reflectivity and (b) group delay response of the realized SFBGs. Solid line: $N = 70, c_{g1} = 1.449 \times 10^{-2}$; dash line: $N = 60, c_{g1} = 1.695 \times 10^{-2}$; dot line: $N = 50, c_{g1} = 2.040 \times 10^{-2}$; dash-dot line: $N = 40, c_{g1} = 2.564 \times 10^{-2}$. In (b), the thin dotted lines represent the fitted curves for all group delay responses.

bandwidth of the SFBG prism. Designing equivalently chirped SFBGs with a larger 3-dB bandwidth and/or using a single sideband modulation scheme are workarounds for this issue.

It can be noted that the group delay responses in Fig. 3 are not exactly linear. The error associated with these responses, while small, will affect the shape of the array factor of the PAA. In order to better understand the influence of this difference, it is necessary to carry out a theoretical error analysis which is presented in Section VI.

VI. Effect of Group Delay Nonlinearities on the Array Factor

Equation (1) presents the array factor of a linearly spaced PAA when a linear time-delay progression is applied to the electrical signals feeding the antenna elements. In a more general sense, the normalized array factor of a PAA with linearly spaced antenna elements can be expressed as follows:

$$\text{af} = \frac{1}{M} \sum_m I_m \, e^{j(m-1)k\,d\,\cos\,\theta} \tag{14}$$

where I_m is the electrical current feeding the mth antenna element, which can be expressed as

$$I_m = A_m \, e^{j\,\beta_m} \tag{15}$$

where A_m and β_m are the amplitude and phase of the electrical current, respectively.

The array factor can, thus, be expressed as

$$\text{af} = \frac{1}{M} \sum_m A_m e^{j[(m-1)\,k\,d\,\cos\,\theta + \beta_m]} \tag{16}$$

We assume a constant amplitude, A, for the electrical signals feeding all antenna elements, and a phase progression given by

$$\beta_m = (m-1)\beta. \tag{17}$$

From (16) and (17), it is possible to arrive at (1). We now introduce the error term in the time delay such as

$$\Delta t_m = (m-1)\,\Delta t + \varepsilon_{t\,m}. \tag{18}$$

We define the phase error as

$$\varepsilon_{\beta\,m} = 2\pi f \varepsilon_{t\,m}.$$

The normalized array factor can thus be expressed as

$$af = \frac{A}{M} \sum_m e^{j[(m-1)\psi + \varepsilon_{\beta\,m}]}. \tag{19}$$

The error in the normalized array factor can be expressed as

$$\varepsilon_{\text{af}} = \frac{A}{M} \sum_m \left[e^{j(m-1)\psi} \left(e^{j\,\varepsilon_{\beta\,m}} - 1 \right) \right]. \tag{20}$$

VII. Experimental Results

The SFBGs detailed in the previous sections have been fabricated and characterized. A 14-cm uniform phase mask has been used in a beam scanning FBG fabrication setup to realize the different superstructures. The SFBGs were written on hydrogen-loaded single-mode fiber (SMF). A sine-square apodization profile was used along the length of the superstructure to minimize the presence of sidelobes in the amplitude spectrum and to reduce the group delay ripple.

To characterize the SFBGs, a vector network analyzer (VNA) and a power meter were used to record the phase and amplitude responses, respectively. A low-frequency electrical signal was used to intensity modulate an optical carrier generated by a TLS. After being reflected by the grating, the modulated optical signal was sent to a PD. The recovered electrical signal was amplified

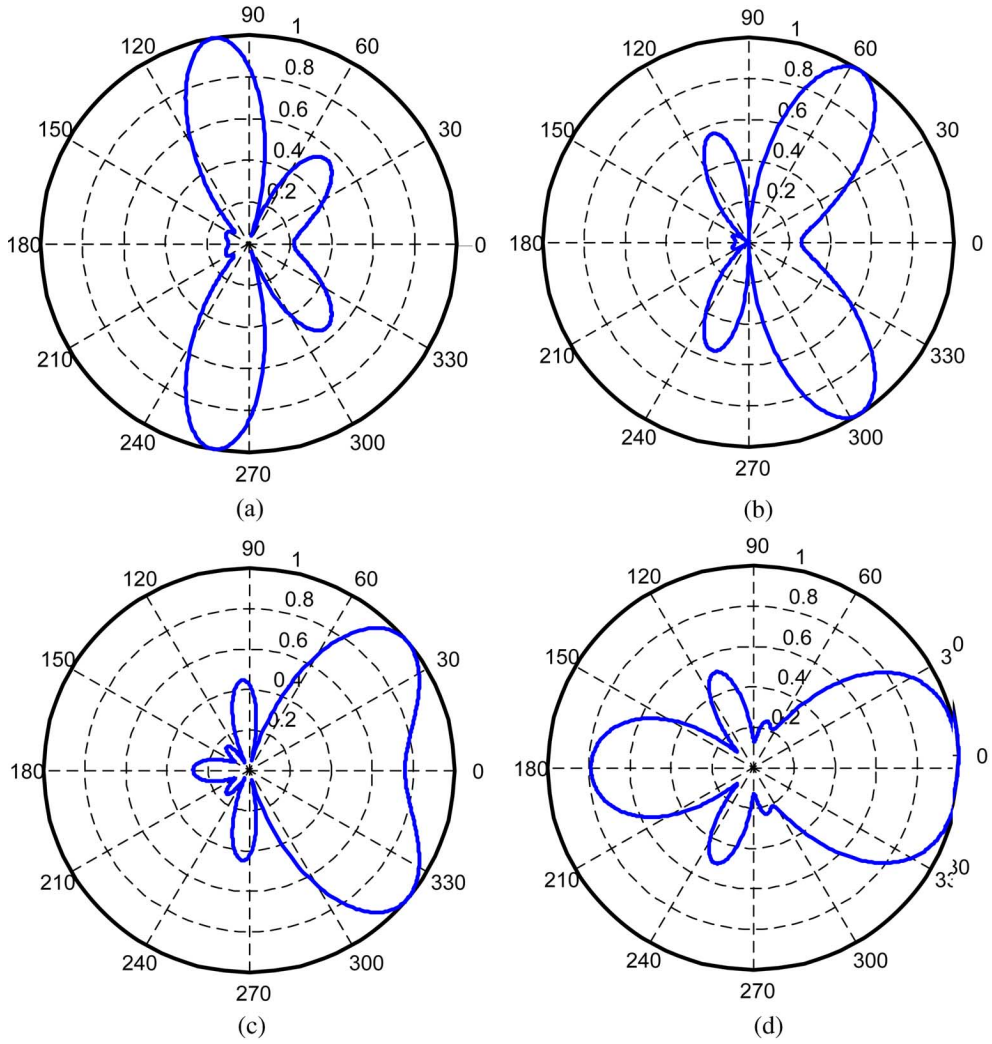

Fig. 5. Simulated array factors for a linear PAA fed with the true time-delay beamformer. The time delays considered are taken from the experimental group delay responses of the SFBGs. For simulation purposes, $s = 7.5$ mm, $M = 4$, and $f_{\mathrm{RF}} = 18$ GHz.

and sent to the VNA. The instruments were controlled via their GPIB bus by a custom-designed software module developed in LabView.

Fig. 4(a) and (b) shows the reflection spectra and the group delay responses of the realized SFBGs. The responses of the fabricated SFBGs match very well with those of the theoretical simulation results. The dispersion of each SFBG, averaged over the 3-dB bandwidth of the -1st-order are as follows: SFBG-1: $d_1 = 520.5$ ps/nm, SFBG-2: $d_2 = 663.0$ ps/nm, SFBG-3: $d_3 = 803.97$ ps/nm, and SFBG-4: $d_4 = 948.2$ ps/nm. The 3-dB bandwidth of all the realized gratings was slightly above 0.38 nm.

We can see from Fig. 4 that the amplitude spectra show a slight ripple. Also, a group delay ripple is present in all grating responses. These differences, as well as the differences between the measured dispersions and the theoretical values can be associated with uncertainties and errors in the fabrication process of the gratings. From Fig. 4(b), we can see that the group delay responses of the SFBGs overlap at lower wavelengths. Because of this, the usable range of the TTD beamformer is limited to outside of this region.

Fig. 5 shows simulated array factors for a linear phased array antenna system based on the proposed TTD beamformer. The time delays considered are experimental data points taken from the group delay response of the SFBGs. As can be seen, the main lobe of the array factor can be steered in over a large range (from 0° to 100°). The linear array of elements of the PAA is considered to be along the axis 0 °–180 °. For simulation purposes, the distance between the elements s was set at 7.5 mm, the RF frequency was 18 GHz, and a single sideband modulation scheme is considered.

The group delay responses presented in Fig. 4 are not completely linear. A group delay ripple is present in all responses, which will affect the shape of the PAA array factor. Based on the analysis of Section VI, the error associated with the main lobe of the array factor with respect to a theoretical array factor based on ideal time delays, as a function of the optical carrier wavelength is shown in Fig. 6. It can be noted that the error is confined within $\pm 10°$ with larger errors towards the lower wavelength. This is expected as the time delay progression at lower wavelengths was designed to be small and a slight variation in the group delay response will produce larger errors in the main

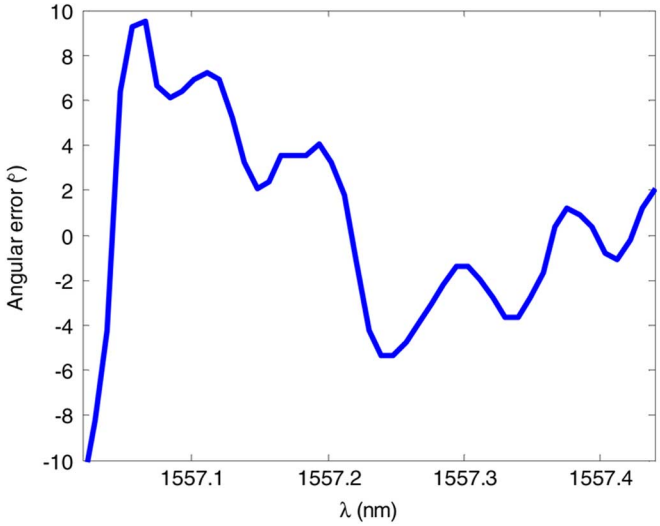

Fig. 6. Error in the orientation of the main lobe of the array factor as a function of the optical carrier wavelength.

lobe orientation. The error is quickly reduced to $\pm 5^\circ$ at around 1557.10 nm and above.

VIII. Conclusion

A photonic TTD beamforming system for PPAs based on SFBGs with linearly increasing equivalent chirps has been proposed and demonstrated. The theory behind SFBGs with equivalent chirps was detailed and a closed-form equation for the equivalent dispersion was presented for the first time. A theoretical analysis of the influence of errors in the group delay response on the array factor has been presented. Experimental spectra and group delay responses of the SFBGs have been presented. Theoretical array factors, simulated based on the experimental data have shown for different operating points of the photonic beamformer. Finally, an analysis of errors in the experimental group delay responses and their impact on the array factor has been presented. The errors are limited to $\pm 10^\circ$ over the entire band of operation and are quickly limited to $\pm 5^\circ$ at around 1557.10 nm and above.

References

[1] O. Raz, R. Rotman, Y. Danziger, and M. Tur, "Implementation of photonic true time delay using high-order-mode dispersion compensating fibers," *IEEE Photon. Technol. Lett.*, pp. 1367–1369, May 2004.

[2] D. Dolfi, D. Mongardien, S. Tonda, M. Schaller, and J. Chazelas, "Photonics for airborne phased array radars," in *Proc. IEEE Int. Conf. Phased Array Syst. Technol.*, May 2000, pp. 379–382.

[3] R. A. Minasian and K. E. Alameh, "Optical-fiber grating-based beamforming network for microwave phased arrays," *IEEE Trans. Microw. Theory Tech.*, vol. 45, no. 8, pp. 1513–1517, Aug. 1997.

[4] L. Xu, R. Taylor, and S. R. Forrest, "The use of optically coherent detection techniques for true-time delay phased array and systems," *J. Lightw. Technol.*, vol. 13, no. 8, pp. 1663–1678, Aug. 1995.

[5] Y. Chen and R. T. Chen, "A fully packaged true time delay module for a K-band phased array antenna system demonstration," *IEEE Photon. Technol. Lett.*, vol. 14, no. 8, pp. 1175–1177, Aug. 2002.

[6] D. N. McQuiddy, Jr., R. L. Gassner, P. Hull, J. S. Mason, and J. M. Bedinger, "Transmit/receive module technology for X-band active array radar," *Proc. IEEE*, vol. 79, no. 3, pp. 308–341, Mar. 1991.

[7] R. Rotman, O. Raz, and M. Tur, "Requirements for true time delay imaging systems with photonic components," in *Proc. IEEE Int. Symp. Phased Array Syst. Technol.*, Oct. 2003, pp. 193–198.

[8] P. M. Freitag and S. R. Forrest, "A coherent optically controlled phased array antenna system," *IEEE Microw. Guided Wave Lett.*, vol. 3, no. 9, pp. 293–295, Sept. 1993.

[9] W. Ng, A. A. Walston, G. L. Tangonan, J. J. Lee, I. L. Newberg, and N. Bernstein, "The first demonstration of an optically steered microwave phased array antenna using true-time-delay," *J. Lightw. Technol.*, vol. 9, no. 9, pp. 1124–1131, Sep. 1991.

[10] I. Y. Lee, K. H. Lee, D. Y. Kim, Y. Y. Kim, and J. H. Yea, "A novel compact multi line phase shifter for precise array antenna beam control," in *Proc. IEEE MTT-S Int. Microw. Symp. Dig.*, Jun. 2004, vol. 3, pp. 1773–1776.

[11] R. S. Chu, K. M. Lee, and A. T. S. Wang, "Multiband phased-array antenna with interleaved tapered-elements and waveguide radiators," in *Proc. Antennas Propag. Soc. Int. Symp.*, Jul. 1996, vol. 3, pp. 1616–1619.

[12] S. Tang, R. T. Chen, B. Li, and J. Foshee, "Waveguides take to the sky," *IEEE Circuits Dev. Mag.*, vol. 16, no. 1, pp. 10–16, Jan. 2000.

[13] H. Zmuda, R. A. Soref, P. Payson, S. Johns, and E. N. Toughlian, "Photonic beamformer for phased array antennas using a fiber grating prism," *IEEE Photon. Technol. Lett.*, vol. 9, no. 2, pp. 241–243, Feb. 1997.

[14] O. Raz, S. Barzilay, R. Rotman, and M. Tur, "Fast switching and wideband photonic beamformer with flat RF response and squintless scan performance," in *Proc. Opt. Fiber Commun. Conf.*, Anaheim, CA, Mar. 2007, paper OWU3.

[15] D. B. Hunter, M. E. Parker, and J. L. Dexter, "Demonstration of a continuously variable true-time delay beamformer using a multichannel chirped fiber grating," *IEEE Trans. Microw. Theory Tech.*, vol. 54, no. 2, pp. 861–867, Feb. 2006.

[16] I. Frigyes and A. J. Seeds, "Optically generated true-time delay in phased-array antennas," *IEEE Trans. Microw. Theory Tech.*, vol. 43, no. 9, pp. 2378–2386, Sep. 1995.

[17] Y. Liu, J. Yang, and J. P. Yao, "Continuous true-time-delay beamforming for phased array antenna using a tunable chirped fiber grating delay line," *IEEE Photon. Technol. Lett.*, vol. 14, no. 8, pp. 1172–1174, Aug. 2002.

[18] M. Bass and E. W. Van Stryland, *Fiber Optics Handbook*. New York: McGraw-Hill, 2002.

[19] Y. Liu and J. P. Yao, "Wideband true time-delay beamformer employing a tunable chirped fiber grating prism," *Appl. Opt.*, vol. 42, no. 13, pp. 2273–2277, May 2003.

[20] Y. Liu, J. P. Yao, and J. Yang, "Wideband true-time-delay unit for phased array beamforming using discrete-chirped fiber grating prism," *Opt. Commun.*, vol. 207, no. 1–6, pp. 177–187, Jun. 2002.

[21] X.-F. Chen, X.-H. Li, L. Xia, S.-Z. Xie, C.-C. Fan, and J.-P. Want, "Experimental investigation of a sampled grating with a chirp in the sampling period," *Microw. Opt. Technol. Lett.*, vol. 29, no. 2, pp. 128–130, Apr. 2001.

[22] X.-F. Chen, Y. Luo, C.-C. Fan, T. Wu, and S.-Z. Xie, "Analytical expression of samples Bragg gratings with chirp in the sampling period and its application in dispersion management design in a WDM system," *IEEE Photon. Technol. Lett.*, vol. 12, no. 8, pp. 1013–1015, Aug. 2000.

[23] T. Erdogan, "Fiber grating spectra," *J. Lightw. Technol.*, vol. 15, no. 8, pp. 1277–1294, Aug. 1997.

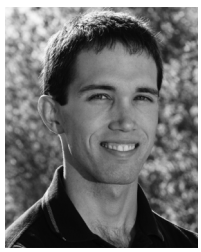

Sebastien Blais (M'01) received the B.A.Sc. degree from the Université de Moncton, Moncton, Canada in 2003, and the M.S. degree in electrical engineering from the University of Ottawa, Ottawa, Canada, in 2005.

Since completing his M.S. degree, he has been working toward the Ph.D. degree at the UMicrowave Photonics Research Laboratory, School of Information Technology and Engineering, University of Ottawa. His research interests include fiber Bragg gratings, superstructured fiber Bragg gratings, photonic processing of microwave signals, optical waveguide devices, and phased array antennas.

Jianping Yao (M'99-SM'01) received the Ph.D. degree in electrical engineering in 1997 from the Université de Toulon, Toulon, France.

He joined the School of Information Technology and Engineering, University of Ottawa, Ontario, Canada, in 2001, where he is currently a Professor, Director of the Microwave Photonics Research Laboratory, and Director of the Ottawa-Carleton Institute for Electrical and Computer Engineering. From 1999 to 2001, he held a faculty position with the School of Electrical and Electronic Engineering, Nanyang Technological University, Singapore. He spent three months as an invited professor with the Institut National Polytechnique de Grenoble, France, in 2005. His research has focused on microwave photonics, which includes all-optical microwave signal processing, photonic generation of microwave, mm-wave and THz, radio over fiber, UWB over fiber, fiber Bragg gratings for microwave photonics applications, and optically controlled phased array antenna. His research interests also include fiber lasers, fiber-optic sensors, and biophotonics. He has authored or coauthored approximately 200 papers in refereed journals and conference proceeding.

Dr. Yao is an Associate Editor of the *International Journal of Microwave and Optical Technology*. He is on the Editorial Board of the IEEE TRANSACTIONS ON MICROWAVE THEORY AND TECHNIQUES. He received the 2005 International Creative Research Award of the University of Ottawa. He was the recipient of the 2007 George S. Glinski Award for Excellence in Research. He was named University Research Chair in Microwave Photonics in 2007. He is a registered professional engineer of Ontario. He is a member of SPIE, OSA, and a senior member of the IEEE/LEOS and IEEE/MTT societies.